The Thermal and Mechanical Behavior of Poly(ethylene terephthalate) Fibers Incorporating Novel Thermotropic Liquid Crystalline Copolymers

SCOTT JOSLIN, WOODWARD JACKSON, and RICHARD FARRIS*

Polymer Science and Engineering Department, University of Massachusetts, Amherst, MA 01003

SYNOPSIS

This investigation explores the potential of improving the performance of poly(ethylene terephthalate) fibers by incorporating novel thermotropic liquid crystalline copolymers. Fibers were obtained by melt extrusion and the effect of processing conditions, i.e., spinning temperature, stretch ratio, and post treatment evaluated. The fibers were tested for mechanical performance, dimensional instability (shrinkage), and the development of shrinkage stresses. A segmented block copolymer consisting of rigid-rod, diad, and flexible coil segments was found to improve the performance of poly(ethylene terephthalate) (PET) fibers. At a concentration of 20 wt %, the alternating block copolymer increased the tensile modulus of the fibers by 40% and decreased free shrinkage by 20% compared to neat PET.

INTRODUCTION

In situ composites are formed by the inclusion of a liquid crystalline rigid rod polymer in an isotropic matrix. Kiss[1] used the term *in situ composites* for these materials, since the reinforcing species is not actually present in the starting materials but comes into existence during processing. These systems may provide good mechanical performance while preventing technical difficulties associated with the presence of a solid filler. Solid fillers such as chopped glass fibers can cause significant wear on processing equipment, increase the molten polymer viscosity, and pose difficulties in compounding. Thus it would be highly desirable to develop *in situ* composites, since the reinforcing component develops upon solidification into highly oriented and rigid inclusions.

Thermotropic liquid crystalline polymers (TLCPs) are currently the preferred reinforcement material for designing *in situ* composites. The large-scale interest in thermotropic systems is due to their ability to be used with conventional melt processing techniques and equipment without expensive and potentially hazardous solvents. Thermotropic polymers can form highly oriented, anisotropic fibrous domains or inclusions in a matrix polymer when processed under the appropriate conditions. Due to their potential to develop high strength and stiffness, these fibrous inclusions may act as a reinforcement agent, much like chopped glass. Furthermore TLCPs offer a range of other interesting properties such as low viscosity, low thermal expansion in the direction of orientation, and chemical resistance. Thus TLCPs blended with engineering thermoplastics could impart thermal stability or function as a processing aid.[2-5] Most of the work to date has centered on melt blending commercial thermotropic copolyesters, such as Vectra®, Xydar®, or X7G®, with engineering thermoplastics, e.g., poly(ethylene terephthalate) (PET) or poly(butylene terephthalate) (PBT), as well as polycarbonate (PC), poly(ether ether ketone) (PEEK) and nylons. Several reviews on the subject have been published recently.[6-8]

A degree of compatibility between TLCPs containing ethylene terephthalate units with PET and polycarbonate has been observed, but the majority of thermoplastics have been found to be incompatible with TLCPs.[9,10] Incompatibility between blend components is thought to be undesirable since it

* To whom correspondence should be addressed.

Journal of Applied Polymer Science, Vol. 54, 439–455 (1994)
 CCC 0021-8995/94/040439-17

can result in poor interfacial adhesion and adversely affect the mechanical properties of the system.[1,11,12] However, miscibility is also thought to be undesirable for these blends. The existence of a two-phase morphology is regarded as necessary in order to obtain the processing and mechanical benefits of the TLCP. Thus a degree of compatibility is desired such that good interfacial adhesion is achieved without sacrificing potential processing and property enhancements. An approach for accomplishing this objective is the use of tailored block copolymers. By incorporating flexible blocks similar to the matrix polymer into the TLCP chain, the interfacial adhesion between blend components should improve and consequently increase mechanical performance.

In this study, PET has been blended with several novel thermotropic liquid crystalline polyesters and the physical and mechanical properties investigated. The objective was to determine if properties superior to neat PET fibers could be attained by incorporating a liquid crystalline polyester composed of rigid mesogenic moieties and flexible PBT segments. PBT is miscible with PET and could promote compatibility between the two phases.

Due to limited amounts of the block copolymers, a screening procedure has been developed to determine whether a blend system exhibits desirable characteristics. Compositions varying from 5 to 20 wt % LCP are commercially interesting; therefore, evaluations focused on this range. Fibers were prepared by melt extrusion followed by cold and hot drawing, then tested for tensile performance, dimensional instability (shrinkage), and the development of shrinkage stresses.

MATERIALS

The thermotropic LCPs used in this study are a group of novel block copolymers kindly synthesized by Drs. Lenz and Kantor's group at the University of Massachusetts, Amherst.[13] The LCPs are segmented block copolymers consisting of rigid-rod, diad, and flexible coil segments. Figure 1 shows a

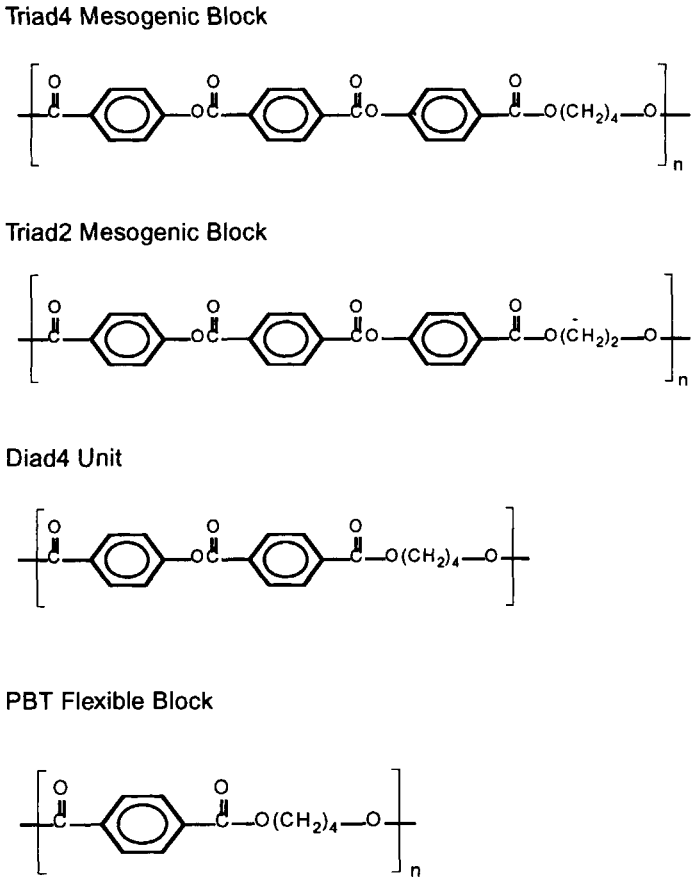

Figure 1 The rigid and flexible moieties incorporated into the alternating block copolymers.

schematic of the general structures used in this study. The mesogenic blocks are composed of either poly(tetramethylene-4,4′ terephthaloyl dioxydibenzoate) (Triad4) or poly(dimethylene-4,4′ terephthaloyl dioxydibenzoate) (Triad2) units. The flexible coil segments are poly(butylene terephthalate) (PBT). Furthermore, due to the reaction scheme chosen to synthesize these copolymers, tetramethylene-4.4′ dioxyterephthaloyl benzoate (Diad4) sequences are incorporated between the rigid-rod and flexible coil segments. These diads are known to be mesogenic.[14]

Several different copolymer systems have been investigated to determine the optimum molecular architecture necessary for PET reinforcement. Variables that were considered included: block size, rigid-rod content, PBT content, and mesogen rigidity. The molar ratio of the Diad4, Triad, and PBT sequences incorporated into each block copolymer are shown in Figure 2. For instance the Triad4 (2 : 4 : 21) block copolymer has two Diad4 units which separate Triad4 and PBT blocks having segment lengths of 4 and 21 units, respectively.

The amount of material available for blending and property determination for each LCP was limited to approximately 7 grams, thus the mechanical properties of the neat copolymers could not be determined.

The fiber grade PET used in this study was kindly provided by the Akzo Corp. The material had a reported melting transition of 273°C and an inherent viscosity of 2.04 (dl/g). The PET was blended as received without further purification.

EXPERIMENTAL

Thermal Characterization

The transition temperatures of the liquid crystalline block copolymers were measured calorimetrically using a TA Instruments 2910 differential scanning calorimeter. Temperature calibration was performed using an indium standard. Samples of approximately 10 mg were initially heated in a nitrogen atmosphere from 30°C to 300°C at a heating rate of 20°C/min, followed by quenching with liquid nitrogen. Samples were then reheated to 350°C at a heating rate of 20°C/min. The reported transitions are the maxi-

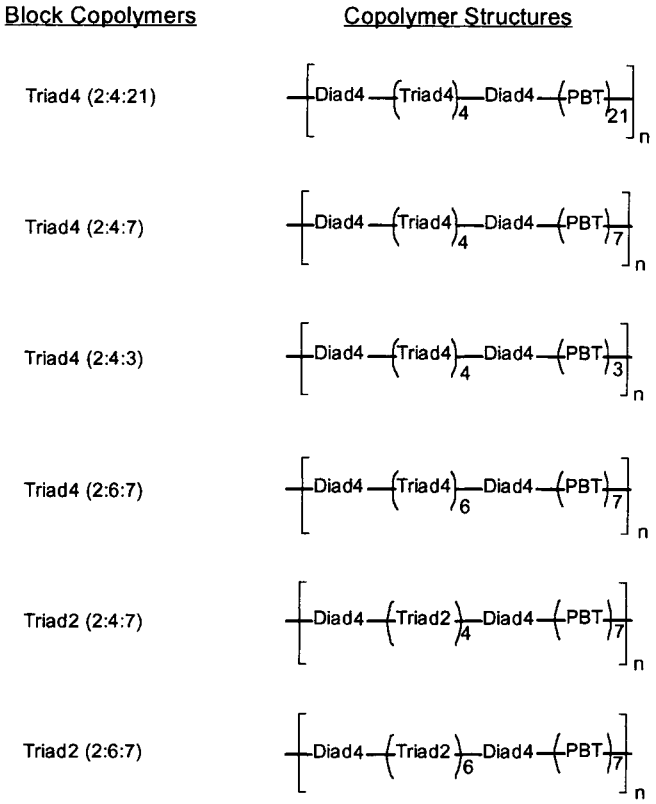

Figure 2 Schematics of the polymer structures and the molar ratios of mesogenic to flexible moieties incorporated into the alternating block copolymers.

mum peak temperatures observed during the second heating run.

The degradation temperatures in air were also measured using a TA Instruments 2950 thermogravimetric analyzer. Samples were scanned from room temperature to 600°C at a heating rate of 20°C/min. The reported degradation temperature corresponds to 0.5% weight loss.

Fiber Formation

Powders of the thermotropic polyesters and PET were tumble mixed for 24 h. The amounts of block copolymer used in the blends were 5, 10, and 20% by weight. The mixed polymer powders were then compression molded using a Carver laboratory press at 270°C for 1 min. The compressed sample was consequently ground in an analytical mill to a particle size of less than 1000 microns and dried at 120°C for a minimum of 24 h. Compression molding followed by grinding was convenient for obtaining particles that effectively fed into the mini-extruder.

Once thoroughly dried, the blends were extruded and spun into fibers. Extrusion was carried out with a ¼-inch Randcastle single screw mini-extruder. The mini-extruder has four temperature zones, which may be varied independently. The feeding, compression, and melting sections (zones one, two, and three, respectively), were set at 220°C, 260°C, and 280°C. The temperature of the die zone was varied to observe the effects on fiber spinning. The main criterion for determining the die temperature was the ability to obtain a uniform melt without die swell. The screw speed was held constant at 30 rpm corresponding to a flow rate of 1.5 g/min and a polymer residence time of two to four minutes within the extruder. The residence time in the extruder was kept to a minimum in order to reduce the possibility of transesterification reaction between the blend components.

Upon exiting the extruder die, the polymer was stretched using a custom-built take-up device. A take-up speed of 75 m/min was used for all systems, which corresponds to an approximate stretch ratio of 300 to 400. The stretch ratio for each system was determined as the ratio between the die and the drawn extrudate cross sections (A_0/A_f). The round-hole capillary die had a diameter of 1575 μm and an aspect ratio of 10. Fiber diameters were determined by optical microscopy.

The heat treatment of PET fibers is an important processing stage that determines the ultimate properties of the material. A two-step posttreatment process was performed immediately following the spinning process. Post drawing was accomplished using a continuous process between optoelectronically monitored feed and take-up spools. Cold drawing was performed at 85°C using a standard laboratory hot plate. The speed of the feed spool was kept constant at 4 m/min while the speed of the take-up winder was continuously monitored and increased until a stable neck was observed. For neat PET this occurred at a draw ratio of 3.5.

Hot drawing was accomplished using a similar procedure at a temperature of 205°C. The maximum draw ratio was determined by slowly increasing the speed of the take-up spool until excessive filament breakage occurred. The speed of the take-up spool was then decreased until drawing could proceed for at least two minutes without filament breakage. For neat PET this corresponded to a maximum hot draw ratio of 1.5 and a total fiber draw ratio of 5. The total draw ratio was calculated as the ratio of the as-spun and final posttreated fiber cross sections. All samples were collected and tested at the maximum draw ratio unless otherwise specified.

Tensile Testing

Tensile tests were performed on an Instron 1113 tensile tester connected to a personal computer. In order to facilitate mounting and alignment, specimens were affixed to paper tabs. Fiber diameters were measured using an Olympus microscope equipped with a calibrated scale accurate to ± 0.5 μm. A minimum of five diameter measurements per fiber were obtained. The applied strain rate was 10% elongation per minute, with an initial gauge length of 50 mm. A 550g Toyo TI550 load cell measured the fiber load. The Young's modulus was determined from the best linear fit through the initial region of the stress–strain curve. Instrument compliance was measured and the apparent modulus was found to be approximately 2% lower than the true modulus. Samples that exhibited grip failure were omitted from the tenacity and ultimate elongation results. Each tensile property was averaged over nine tests and performed at ambient conditions in the laboratory. Standard deviations ranged from 5 to 10% for each system.

Thermal Instability

Shrinkage experiments were performed by placing the fibers in a convection oven preheated to 190°C for 15 min. Prior to heating, the fibers were conditioned for 24 h at 21°C and 68% relative humidity. The sample lengths before and after heating were

determined at ambient temperature by straightening the fibers with a small load and measuring the initial (L_0) or final (L_1) length respectively. All samples were approximately 20 cm in length before testing. After removal from the oven, the fibers were reconditioned for one hour and the resultant dimensional changes determined. The free shrinkage was computed as

$$\text{Shrinkage}\,[\%] = (L_0 - L_1)/L_1 * 100.$$

Shrinkage values were averaged over 5 measurements.

To measure the development of shrinkage stresses, force-temperature experiments were carried out using a TA Instruments 2940 thermal mechanical analyzer (TMA). This technique applies a constant strain and measures the development of thermal stresses with temperature change. The fibers were placed in the TMA and an initial strain of 0.05% imposed on the samples. The temperature was then increased at 5°C/min to 190°C and the resultant load monitored. After being held at 190°C for 15 min, the fiber was slowly cooled to room temperature and the shrinkage stresses at 190°C and 30°C recorded.

Morphology

The morphology of the blends was investigated by optical microscopy (OM) and scanning electron microscopy (SEM). Fiber cross sections were prepared by mounting the samples in an epoxy matrix and fracturing the sample after cooling in liquid nitrogen. Fibers were also etched with a 60 parachlorophenol/40 tetrachloroethane mixture to remove the PET. The solvent mixture was slowly dropped onto the fibers at 5 ml per minute for approximately 1 min. All SEM samples were mounted on aluminum stubs, sputtered with gold using an SPE Sputter Coater, and characterized using a JEOL [JSM-35C] scanning electron microscope. An accelerating voltage of 20 kV was used. An Olympus microscope equipped with a Linkam hot stage was used for observing the blends before and after processing.

RESULTS AND DISCUSSION

Thermal Behavior

The results of differential scanning calorimetry (DSC) and thermogravimetric analysis (TGA) scans for the four different block copolymers containing the Triad4 mesogen are presented in Table I. Variables that were investigated included wt % rod content, PBT block size and rod block size. To determine the wt % rod content incorporated into each block copolymer, the rigid portions of the Triad and Diad sequences were accounted for but not the methylene flexible spacers.

These block copolymers exhibit two thermal transitions and a complex phase behavior. The initial transition point (T_m1) corresponds to the melting of PBT blocks and the crystalline to nematic transition of the diad moieties. The diad moieties are mesogenic and optical microscopy reveals that after this transition the polymers are triphasic exhibiting isotropic, nematic, and crystalline phases. (See Figure 3.) The second transition (T_m2) corresponds to the diad moieties becoming isotropic and the crystalline to nematic transition of the Triad mesogenic units.[15] For all of the Triad4 systems this transition occurred around 281°C. The temperature of this transition was independent of the mesogen content in the system.

The first transition temperature (T_m1) corresponds very well with the amount of PBT incorporated into the polymer. Triad4 (2 : 4 : 21) had the largest PBT blocks and the highest initial transition temperature at 214°C. Decreasing the block size to 7 units in the Triad4 (2 : 4 : 7) and Triad4 (2 : 6 : 7) systems dropped the initial transition points to 202°C and 205°C, respectively. Shortening the PBT block size to 3 units in the Triad4 (2 : 4 : 3) polymer further decreased the first transition to 197°C. This trend was not unexpected, since longer PBT segments should permit the formation of crystallites with fewer defects and thus a higher melting temperature. Decreasing the length of PBT segments increases the number of defects in the crystallite structure and lowers the transition temperature. This trend may continue until a critical length is reached, whereupon crystallization is no longer possible or melting is undetectable by DSC.

Table I Thermal Characteristics of the Various Block Copolymers

	T_m1 (°C)	T_m2 (°C)	T_d (°C)	Wt. % Mesogen
Triad4 (2 : 4 : 21)	214	279	291	30
Triad4 (2 : 4 : 7)	202	282	302	49
Triad4 (2 : 4 : 3)	197	282	315	66
Triad4 (2 : 6 : 7)	205	281	336	55
Triad2 (2 : 4 : 7)	195		328	51
Triad2 (2 : 6 : 7)	193		336	57

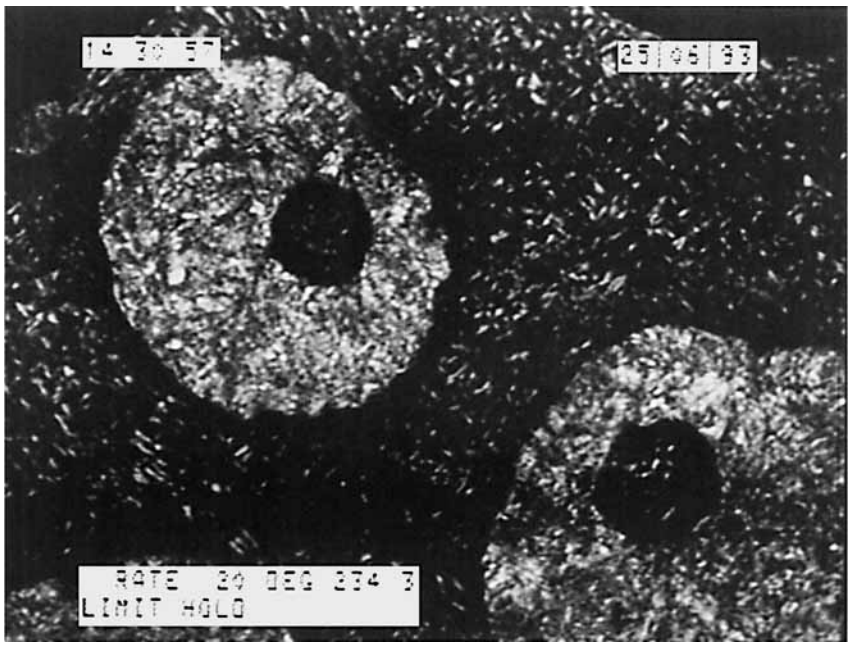

Figure 3 Optical micrograph of the Triad4 (2 : 4 : 7) block copolymer melt above the initial transition point (Tm1). Observed with crossed polarizers and magnified 200×.

The degradation temperature (T_d) of these polymers, as determined by TGA, was dependent upon the amount of PBT in the system and the size of the mesogenic block. As the amount of PBT in the polymers was decreased the decomposition temperature increased from 291°C for the 2 : 4 : 21 system to 315°C for the 2 : 4 : 3 polymer. However the variable having the greatest impact on the degradation temperature was the mesogenic block length. Increasing the Triad block length from 4 to 6 units increased the degradation temperature of the polymer from 302°C to 336°C. The reason for this increase is not yet understood, since it cannot be attributed solely to the amount of rigid rod in the block copolymers. For instance, the Triad4 (2 : 4 : 3) polymer has approximately 10% greater rod content than the Triad4 (2 : 6 : 7) polymer but the degradation temperature was 21°C lower.

The Triad2 systems have different transition temperatures when compared to the Triad4 systems, but the trends are similar. The two Triad2 systems investigated have identical PBT block sizes, 7 units, and initial transition temperatures that are very close, i.e., 195°C and 193°C, respectively. Furthermore, increasing the size of the mesogenic block from 4 to 6 units increased the degradation temperature from 328°C to 336°C. A second transition temperature was not detectable for these systems using DSC. Thus the Triad2 segments may be amorphous or the crystalline to nematic transition of the Triad2 crystals is above the degradation temperature of the polymer. The latter explanation is more plausible, since a glass transition temperature was not readily apparent for these copolymers and the Triad2 homopolymer is known to melt at 360°C.[16] Observation of these polymers with an optical microscope equipped with a hot stage reveals that these polymers exhibited a triphasic morphology above the first transition temperature similar to the Triad4 copolymers.

Triad4 Mechanical Performance

The mechanical properties for the hot drawn 20% Triad4/PET blends are shown in Figure 4. It is evident from the tensile data that varying the size of the PBT block has very little effect on the final fiber properties. The Triad4 systems having mesogen block lengths of 4 units all have moduli similar to the PET control, although the Triad4 (2 : 4 : 7) system does exhibit a small increase to 20 GPa. The largest increase in modulus, 21 GPa, was seen when the mesogen block size was increased from 4 to 6 units. This result was unexpected; it was thought that the absolute rod content of the block copolymers would be the controlling variable for achieving improvements in fiber modulus. However, the length of the mesogenic block appears to have a greater

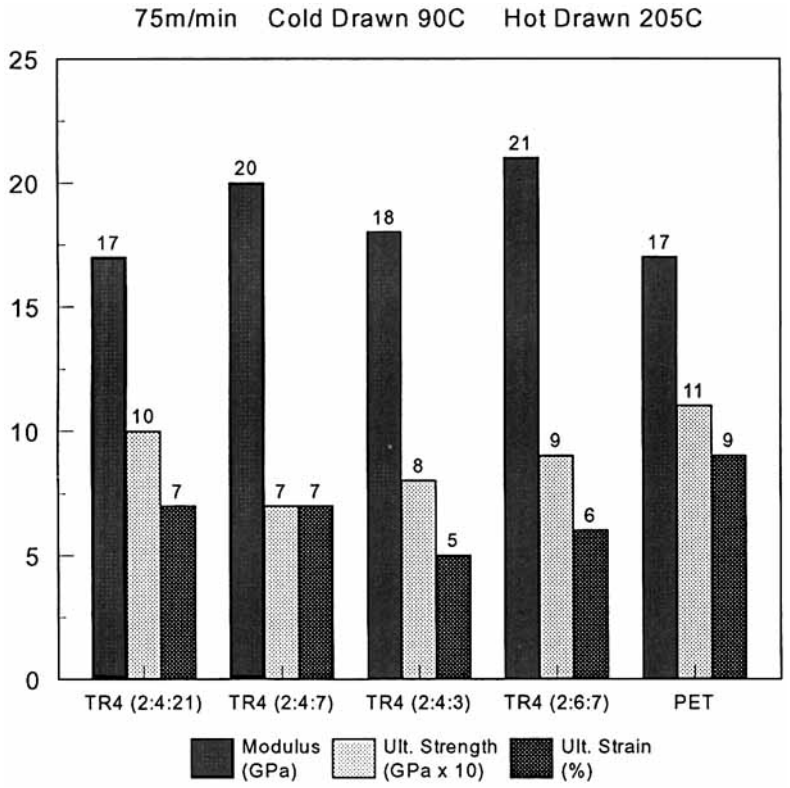

Figure 4 Tensile performance of the hot drawn 20% Triad4/PET blends.

impact on the final fiber stiffness, indicating that a critical mesogenic block length may be necessary to attain maximum reinforcement of the PET matrix.

The ultimate strength and strain to break are slightly lower for the blends when compared to the PET control. However, these properties are not considered crucial when evaluating these materials as potential reinforcing agents for PET. The ultimate strength and strain to break may be influenced by many factors, such as the number of fiber defects and the molecular weight of the TLCPs. These variables are difficult to optimize when screening many different systems with very small quantities of material. Thus the major criterion for determining a system's effectiveness at this juncture is the fiber modulus, since this quantity is less sensitive to processing variables.

To determine the effect of TLCP concentration on the moduli of the fibers, blends of 5, 10, and 20 wt % LCP were evaluated. The results are shown in Figure 5. Surprisingly, increasing the percentage of rigid-rod incorporated into the fiber did not appear to have a significant effect on the modulus. The 5 and 10 wt % blends have almost identical properties to the 20% blends. Thus the moduli appear to be independent of the LCP loading level and very consistent for each system. Essentially, low loading levels of the Triad4 (2 : 4 : 7) LCP are just as effective at obtaining small improvements in the fiber modulus as higher loading levels. Loading levels lower than 5 wt % have not yet been evaluated to determine the extent of this phenomena. A trend based on the amount of rod in the system or the length of the PBT unit could not be found. However, the modulus of the Triad4 (2 : 4 : 21) system was slightly lower than either the Triad4 (2 : 4 : 7) or the Triad4 (2 : 4 : 3) systems, suggesting that large flexible blocks may reduce the ability of the block copolymers to improve or maintain fiber performance.

Triad4 Dimensional Instability

The free shrinkage of the 20% Triad4/PET blends is shown in Figure 6. Two clear trends are visible based on the amount of PBT in the block copolymers and the length of the mesogenic segment. As the amount of PBT is increased in the block copolymers, the dimensional stability of the fibers is decreased significantly, from 10% free shrinkage for the Triad4 (2 : 4 : 3) system to 14% for the Triad4 (2 : 4 : 21) system. Thus a high rod content improves the thermal stability of the blends, but comparison to the

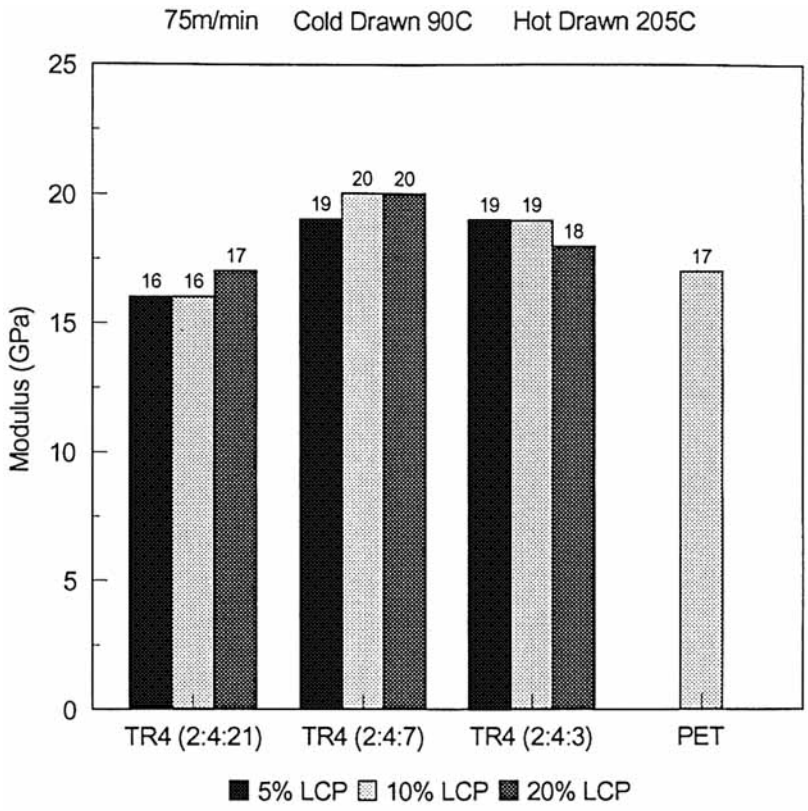

Figure 5 Fiber moduli vs. wt % Triad4 content.

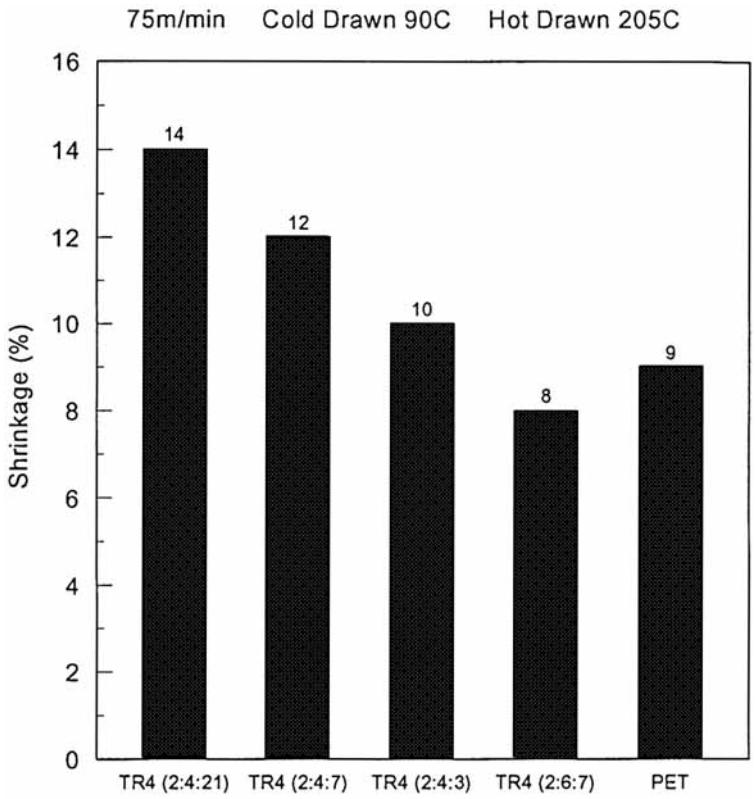

Figure 6 Free shrinkage of the 20% Triad4/PET blends.

PET control reveals no overall improvement in fiber performance. Further improvement in dimensional stability could be obtained by increasing the mesogenic block length from 4 to 6 units. The Triad4 (2 : 6 : 7) system, which exhibited only 8% free shrinkage, was the only Triad4 blend to exhibit increased dimensional stability compared to the PET control. Thus increasing the mesogen block length improved both the mechanical and thermal behavior of the fiber compared to the PET control, while increasing the absolute rod content resulted in only minor performance improvements at best.

Triad2

A slightly stiffer class of block copolymers has also been evaluated for their ability to reinforce PET fibers. These systems are based on the Triad2 mesogenic unit. The Triad2 copolymers are very similar to the Triad4 systems except that two methylene groups have been removed from the mesogen. This should reduce the amount of flexibility incorporated into the mesogenic unit.

Triad2 Mechanical Performance

A comparison of posttreated 20% Triad/PET fiber blends is shown in Figure 7. Both of the Triad2 systems investigated dramatically increased the moduli of the fibers compared to the PET control. The largest increase was seen for the Triad2 (2 : 6 : 7) system which attained a modulus value of 24 GPa. This is a 40% increase over neat PET. Furthermore, a trend that was apparent in the Triad4 systems was also visible in the Triad2 blends, i.e., increasing the length of the mesogenic unit from 4 to 6 units appears to increase the effectiveness of the Triad2 as a reinforcing agent. Increasing the length of the mesogenic block from 4 to 6 units in the Triad4 system increased performance from 20 to 21 GPa respectively, while increasing the block length for the Triad2 systems increased the modulus from 23 to 24 GPa. Although the increase was within experimental error for both the Triad4 and Triad2 systems, the trend is consistent. Comparing the Triad4 and Triad2 systems containing similar block sizes suggests that a 3 GPa increase in fiber moduli may be directly attributed to the increased stiffness of the Triad2 mesogenic unit.

As mentioned previously, the blends' ultimate strength and strain to break are not considered to be determining factors at this juncture of the study. However it is interesting to point out that the Triad2 (2 : 4 : 7) system had a strength of 1300 MPa, which was 200 MPa greater than the PET control. This is important, since it shows that the strength of the fibers can be improved and that the decrease in ultimate strength typically observed for these blends is not an inherent problem with these systems. Thus optimization of synthesis and processing may lead to significantly stiffer and stronger fibers compared to neat PET.

The properties of the Triad2 systems were very sensitive to processing temperatures as shown in Figure 8. Triad2 (2 : 4 : 6) blends were spun at 280°C and 290°C. The 20 wt % blend degraded at 290°C. Gas bubbles were clearly evident, although the TGA indicated the system should have been stable to approximately 328°C. The 5 and 10 wt % systems could be spun at 290°C without visible degradation in the spinning line, but little or no improvement in properties could be detected. Degradation of the polymer may have been facilitated by exposure to high shear fields during extrusion. Thus thermogravimetric analysis may be relied upon only to give an upper bound to degradation when evaluating potential processing conditions. Decreasing the processing temperature to 280°C for the 20% Triad2 (2 : 4 : 7) blend eliminated any visible signs of degradation, improved fiber formation, and led to the large increase in fiber modulus. Due to limited amounts of material, the 5 and 10 wt % blends could not be spun at 280°C. The Triad2 (2 : 6 : 7) blends were all spun at 280°C. The 5 wt % system showed only a minor increase in modulus to 19 GPa but the 10 and 20 wt % blends exhibited significant improvements of 21 and 24 GPa, respectively. Thus there appears to be a definite increase in modulus with concentration, which was the anticipated result. This result is contrary to the mechanical performance of the Triad4 systems, which was independent of the block copolymer concentration. Other processing temperatures were not investigated for the Triad2 (2 : 6 : 7) system.

The effect of draw ratio was investigated for the 20% Triad2 (2 : 6 : 7)/PET blend. The results are shown in Figure 9. As the draw ratio was increased from 4.5 to 5.5 the modulus increased from 18 to 24 GPa, the strength increased from 600 to 900 MPa, and the strain to break decreased from 8 to 5%. These tendencies are typical for drawn samples, i.e., as the amount of orientation is increased in the fibers, the mechanical properties are improved. The trend of increasing strength indicates that these fibers have not been overly drawn. The modulus of excessively drawn fibers may continue to increase slightly but there is a corresponding drop in fiber strength as tie molecules between crystallites are

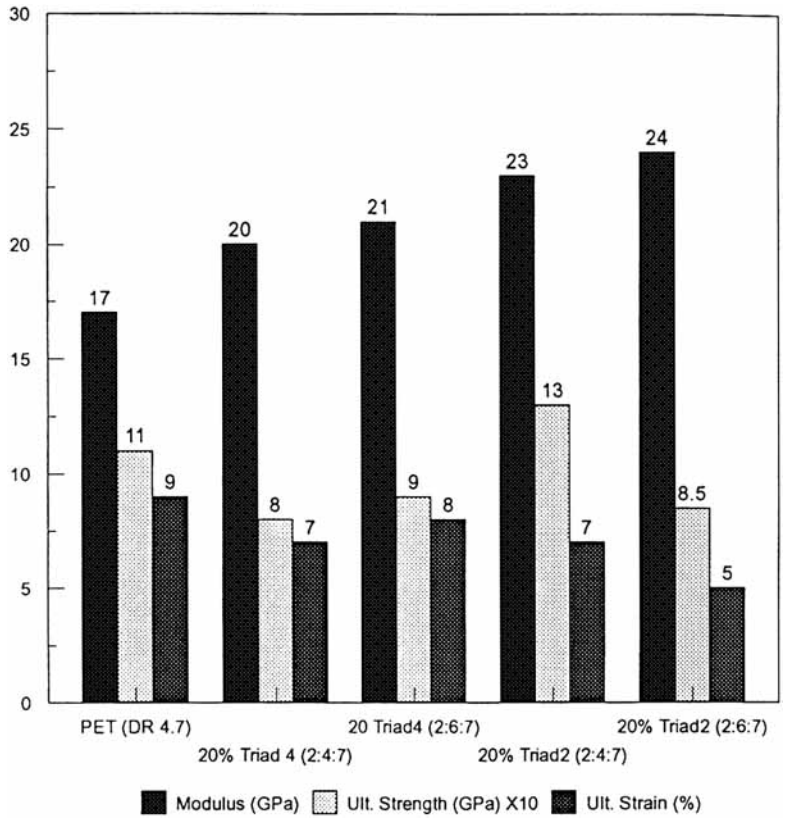

Figure 7 Comparison of the mechanical properties for the 20% Triad4 and Triad2 blends.

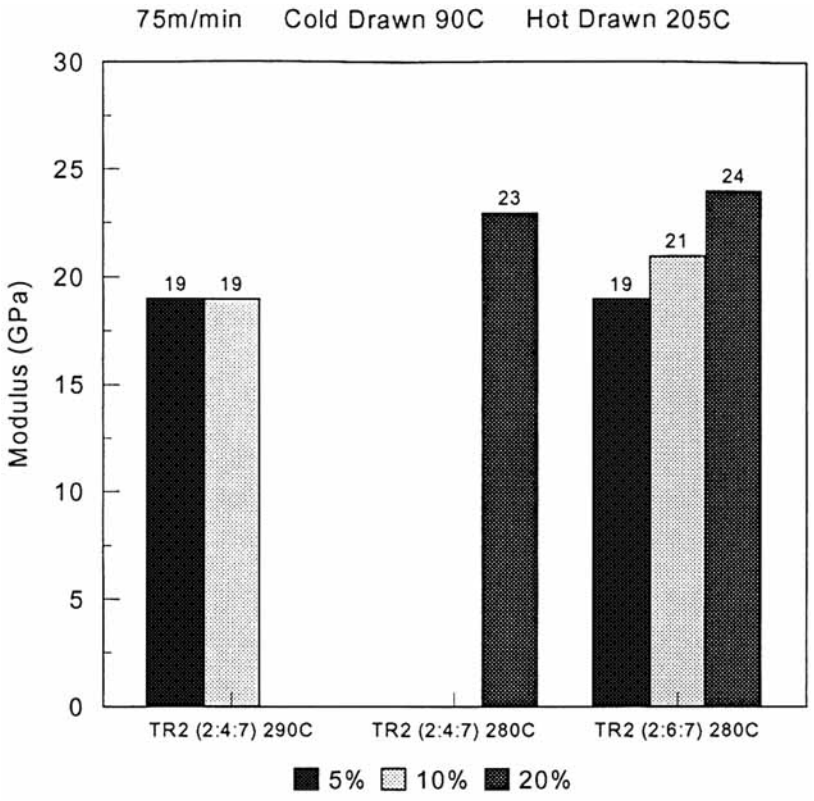

Figure 8 Properties vs. processing for the Triad2 fiber blend systems.

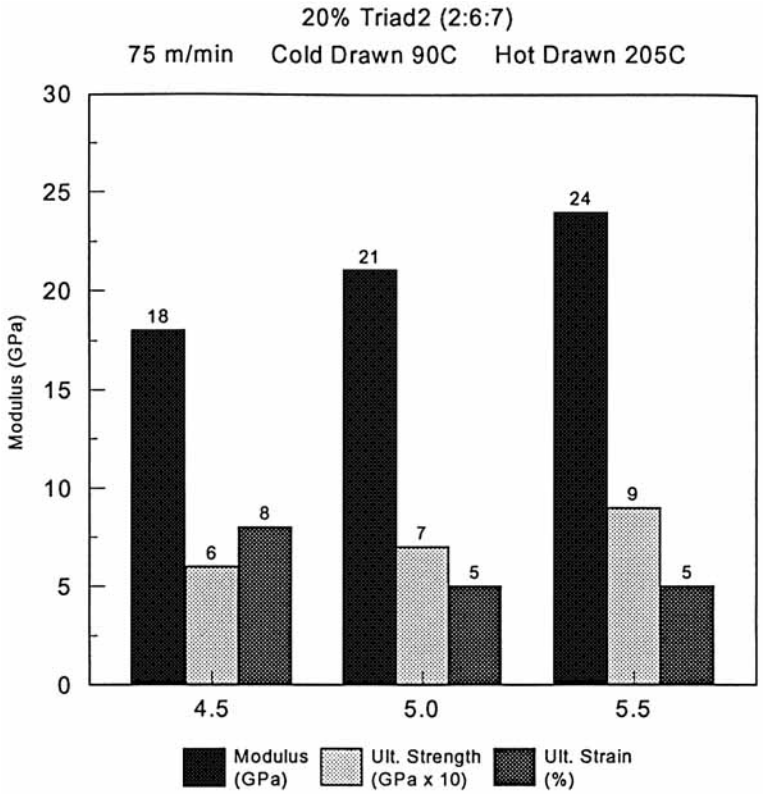

Figure 9 Modulus vs. draw ratio for the 20% Triad2 (2 : 6 : 7) system.

broken.[17] For these fibers a draw ratio beyond 5.5 was not feasible due to frequent fiber breakage in the drawing line. It is important to note that if higher draw ratios can be obtained through process optimization, strengths equivalent or superior to neat PET fibers may be achievable for this system.

Due to limited quantities of the Triad2 (2 : 6 : 7) it has not been possible to determine the mechanical properties of the neat material, but the rule of mixtures can be used to estimate the modulus of the block copolymer. If it is assumed that PET constitutes 80% of the fiber volume and contributes 17 GPa to the composite, a modulus of 52 GPa is obtained for the LCP phase. A stiffness of 52 GPa is in the regime of completely rigid polymers, such as Vectra, and implies that Triad2 (2 : 6 : 7) is indeed a high-performance material. However all of the mechanical properties discussed so far have been for post-treated fibers; when the tensile properties for the as-spun fibers are examined, no increase in tensile performance is observed. Figure 10 shows the moduli-versus-block copolymer content for the 5, 10, and 20 wt % as-spun Triad2 (2 : 6 : 7) fiber blends. All of the as-spun blends exhibit a modulus equivalent to the PET control, 2 GPa, which contradicts the improvements obtained for the post-treated fibers. Thus the rule of mixtures does not apply to the as-spun fibers and Triad2 (2 : 6 : 7) does not improve the tensile performance of PET

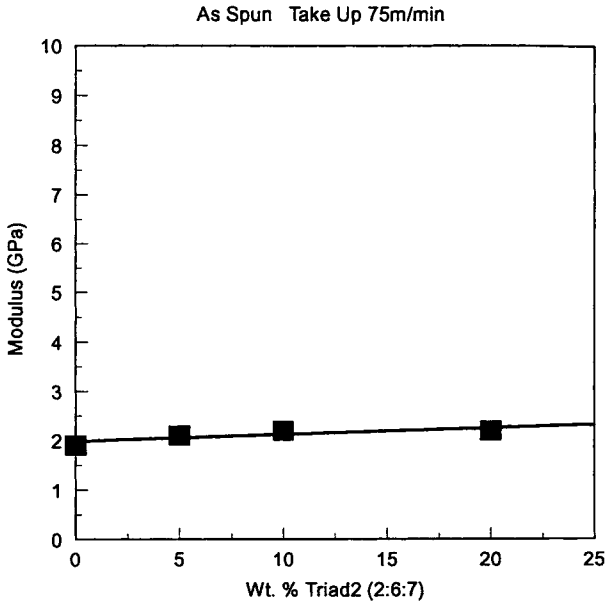

Figure 10 Modulus vs. wt % Triad2 (2 : 6 : 7) content for as-spun fibers.

fibers until after the post-treatment process. This is unusual behavior and suggests that the Triad2 (2 : 6 : 7) may actually be modifying the PET matrix rather than performing as a reinforcement agent. For instance, if the block copolymer increases the orientation or the degree of crystallinity in the PET phase, an improvement in mechanical properties may be obtained. Another possibility is that the block copolymer phase may have been drawn and oriented during the post-treatment process. This is considered a possibility, since the block copolymer is only semirigid and a considerable amount of flexibility has been incorporated into the polymer chain. Increasing the Triad2 (2 : 6 : 7) orientation via the drawing process may have improved the performance of the material to such an extent that mechanical reinforcement was possible.

Triad2 Dimensional Instability

PET fibers are often used in applications where thermal instabilities are undesirable. Fiber instabilities can cause dimensional changes which may ultimately result in the failure of a component. The degree of free shrinkage a fiber incurs at a particular temperature is typically reported as an indicator of its thermal instability. The free shrinkage ($\sigma = 0$) is an important parameter to consider, particularly for applications where fibers are not under dimensional constraints (i.e., clothing, carpets, etc.). However for instances where the fibers are to function under dimensional constraints, such as composites, the development of shrinkage stresses must also be a primary concern. If the free shrinkage of the fiber is reduced but large shrinkage stresses develop upon heating, part warpage could still occur and ultimately result in failure of the composite. Similarly, if fiber shrinkage remained constant but the stress was reduced, warpage might be avoided. Thus if the addition of a liquid crystalline polymer to PET could reduce fiber shrinkage and shrinkage stress, it would be a major advantage for end-use applications. An example of a PET fiber stress–temperature experiment is shown in Figure 11. This technique applies a constant strain, typically 0.05%, and measures the development of thermal stress with temperature change. For a uniaxially constrained sample this can be expressed as

$$d\sigma = -E\alpha dT$$

where σ = stress, E = tensile modulus, α = coefficient of thermal expansion, and T = temperature. Thus if the stress is measured as a function of temperature, the slope will be the product of the modulus and thermal expansion coefficient.

Table II reports the free shrinkage and stress–temperature data for the 20% Triad2 (2 : 6 : 7)/PET blend system at various draw ratios. Only the maximum shrinkage stress obtained at 190°C and the residual stress at 30°C have been reported. Furthermore, the stress-temperature data have been normalized with respect to the initial load applied to the fiber. The PET control had a modulus of 17 GPa and an ultimate strength of 1100 MPa.

The addition of 20% Triad2 (2 : 6 : 7) to PET did reduce the free shrinkage of the fibers. Comparing fiber samples having a maximum shrinkage stress of approximately 80 MPa, the blended fiber exhibited 7% free shrinkage while the PET control

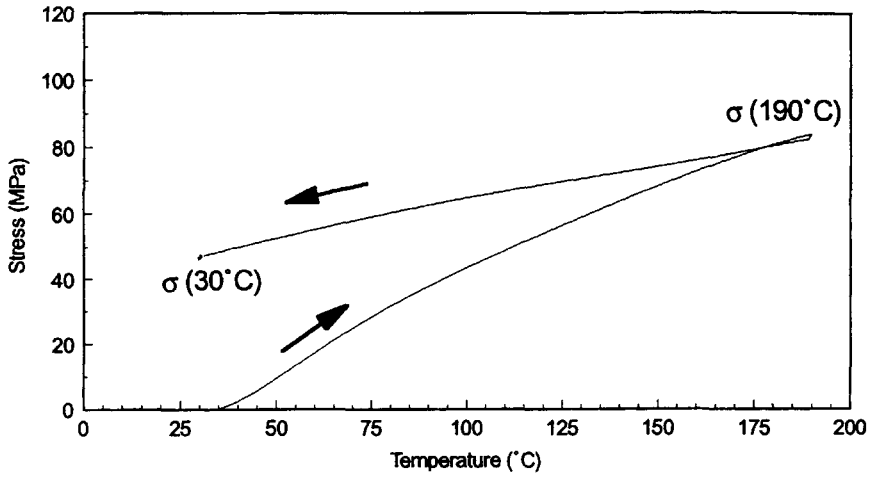

Figure 11 Stress vs. temperature for the PET control fiber having a draw ratio of 5.0.

Table II Dimensional Instability of the 20% Triad2 (2 : 6 : 7) Fiber Blends as a Function of Draw Ratio

	Shrinkage Strain (%)	Shrinkage Stress (MPa)	
		30°C	190°C
PET Draw Ratio = 5.0	9	45	81
20% Triad2 (2 : 6 : 7) Draw Ratio = 4.5	7	37	57
20% Triad2 (2 : 6 : 7) Draw Ratio = 5.0	7	56	84
20% Triad2 (2 : 6 : 7) Draw Ratio = 5.5	8	59	96

had 9%. This is an approximately 30% increase in fiber thermal stability at 190°C. The Triad2 (2 : 6 : 7) also exhibited superior free shrinkage characteristics when compared to the 20% Triad4 (2 : 6 : 7) system which had 8% free shrinkage. Thus the more rigid Triad2 mesogen appears to be more efficient at reducing dimensional instabilities and increasing the mechanical performance of PET fiber.

Although the free shrinkage was reduced in the blended fibers, applying draw ratios ranging from 4.5 to 5.5 increased the maximum shrinkage stress from 57 to 96 MPa. Thus the reduction in free shrinkage may be considered only a partial improvement in thermal stability, since the fiber exhibiting superior tensile performance developed a higher peak shrinkage stress than the PET control.

Both the free shrinkage and the maximum shrinkage stresses in the 20% Triad2 (2 : 6 : 7) blend system were dependent upon the maximum draw ratio experienced by the fiber, a trend that was consistent with the PET control. This indicates that although the free shrinkage of the fibers has been reduced, the mechanisms responsible for dimensional instability in the fiber have not been significantly affected by the addition of the block copolymer. Long and Ward[18] suggest that the peak shrinkage force is due to the retraction of the shortest chains. These chains are thought to control the load-bearing properties, particularly tensile modulus. Thus the higher stiffness, 24 GPa, found in the 20% Triad2 (2 : 6 : 7) system may be the result of a larger number of load-bearing chains in the fiber. This supports the hypothesis that Triad2 (2 : 6 : 7) may be modifying the PET matrix rather than mechanically contributing to the fiber performance as a true reinforcement material.

Triad2 Morphology

Cross sections of 20% Triad2 (2 : 6 : 7) as-spun fibers, observed after fracturing in liquid nitrogen, revealed a distinct two-phase morphology. (See Figure 12.) The LCP phase appears to be evenly distributed throughout the fiber cross-section with the exception of a 1-μm-thick skin region rich in LCP content. (See Figure 13.) Particle size varied and depended upon location within the fiber. Interior particles ranged from 0.5 to 2 μm in diameter, while the particles located in the skin region appeared to have diameters in the range of 0.05 to 0.2 μm. The shape of the LCP phase also varied and appeared to consist of both particulate and elongated geometries. Evidence of adhesion (such as PET residue on the LCP fibrils) was not readily apparent, although the two materials are chemically similar and some interaction between the components was expected. Shin and Chung[19,20] reported excellent adhesion between PET and a thermotropic liquid crystalline polyester when flexible moieties were incorporated into the LCP reinforcement material. The absence of adhesion may be an artifact of the sample preparation technique. For instance, it is well known that cracks tend to propagate along interfaces at liquid nitrogen temperatures. Furthermore, thermal expansion differences between the components may also be a contributing factor.

Figure 14 is an optical micrograph of as-spun 20% Triad2 (2 : 6 : 7) fiber residue magnified 500 times. The PET matrix was removed using a 60/40 parachlorophenol tetrachloroethane mixture, and LCP fibrils could be clearly seen in the fiber residue. This is significant, since it is generally observed that fibrillation of the LCP phase is necessary for good reinforcement of the PET matrix material.[21-24] Furthermore, the presence of a fibrillated Triad2 (2 : 6 : 7) phase indicates that the temperatures selected for processing were reasonable, although they have not been optimized. Fibril formation in LCP-polymer blends depends on many factors such as composition, processing conditions, viscosity ratio of the component polymers, and the rheological characteristics of the matrix polymer.[7] Since only small quantities of the block copolymer were available, a quantitative evaluation of the various processing variables was not possible.

Scanning electron microscopy also confirmed that at least some of the LCP phase was fibrillar and oriented along the fiber axis. (See Figure 15.) The diameters of observed fibrils were approximately 1 to 2 μm and aspect ratios varied from 25 to 160. These aspect ratios are considerably smaller than

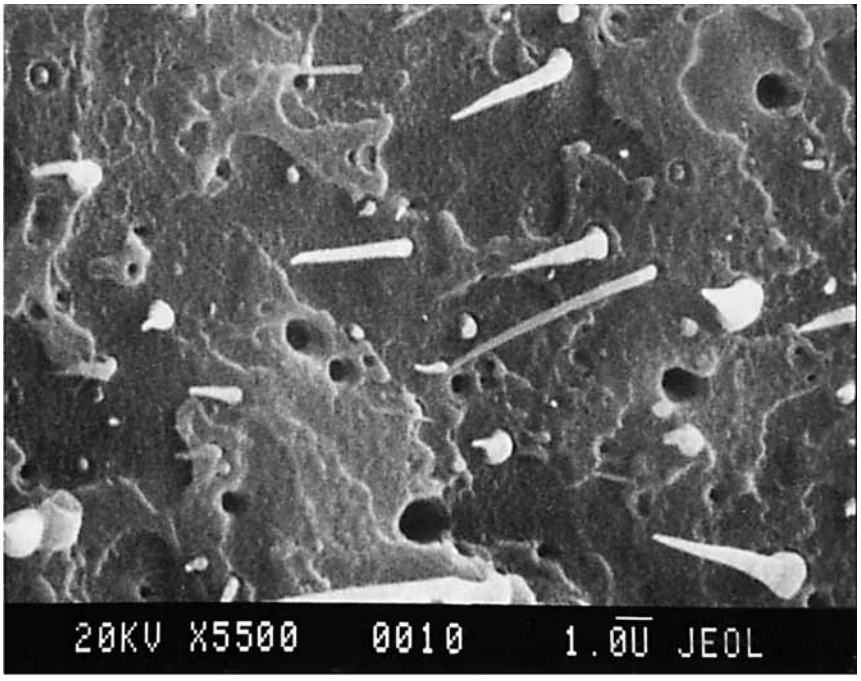

Figure 12 Fiber cross section of an as-spun 20% Triad2 (2 : 6 : 7) blend fiber.

those reported by other investigators, and the number of fibrils was far less than would have been expected for an immiscible 20 wt % blend.[11,25,26] Thus the Triad2 (2 : 6 : 7) may be partially miscible with the PET and/or the geometry of the LCP phase may have been predominately particulate. Partial miscibility of the Triad2 (2 : 6 : 7) with the PET matrix can make fibril generation difficult, and a

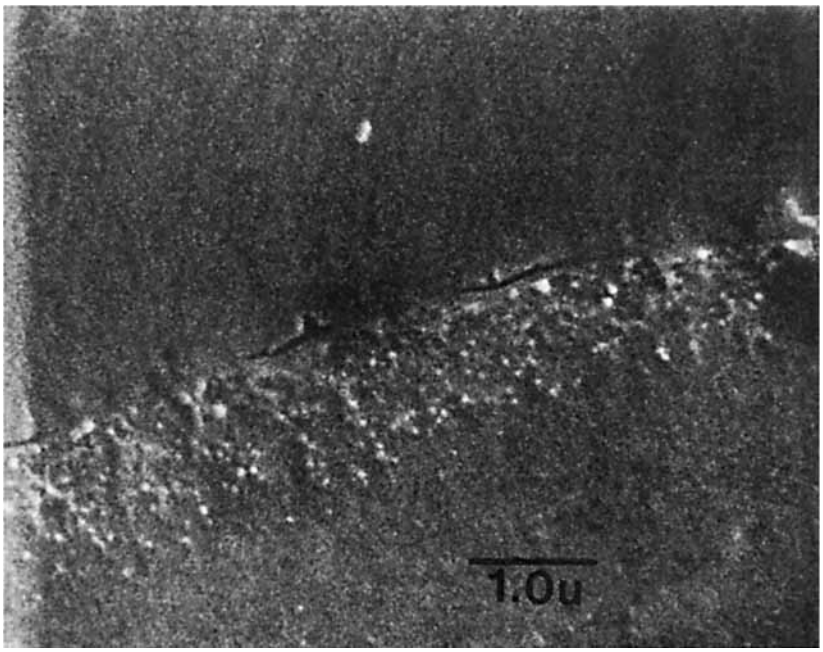

Figure 13 SEM evidence of a skin-core morphology present in the as-spun 20% Triad2 (2 : 6 : 7) fiber.

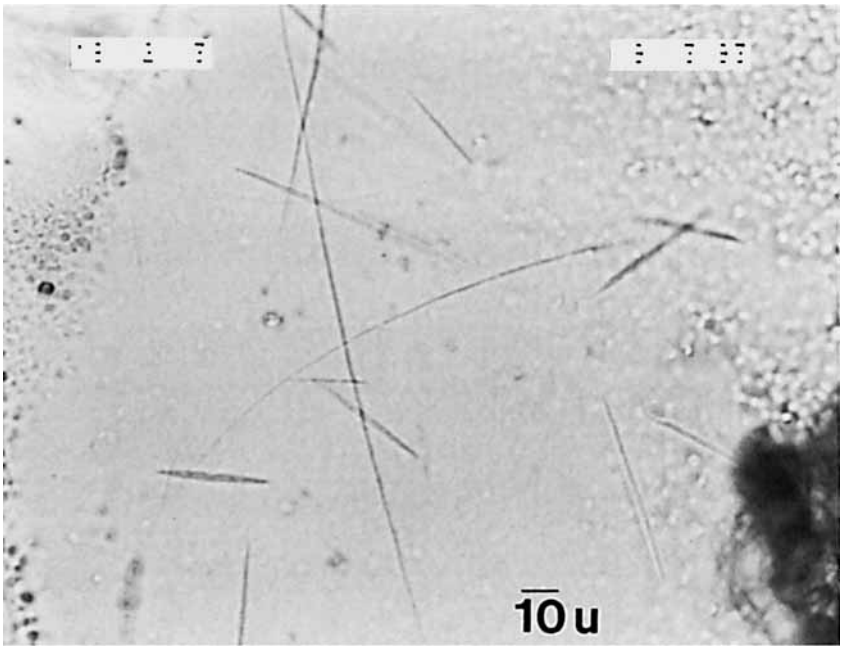

Figure 14 Optical microscopy evidence of fibril formation in the 20% Triad2 (2 : 6 : 7) fiber after etching the PET matrix.

particulate morphology would not be readily visible with optical microscopy since it may have been susceptible to removal during the etching process.[27] Furthermore, if the LCP particles were present but coated/covered with PET, scanning electron microscopy would be unable to distinguish between the two phases.

Comparison of the etched blend fiber with the etched PET control shown in Figure 16 does reveal a dramatic difference in fiber morphology after etching. The PET fiber is smooth and etches evenly, while the blend fiber has a very porous, rough surface structure. This difference in blend fiber structure may be due to particulates of the LCP phase being

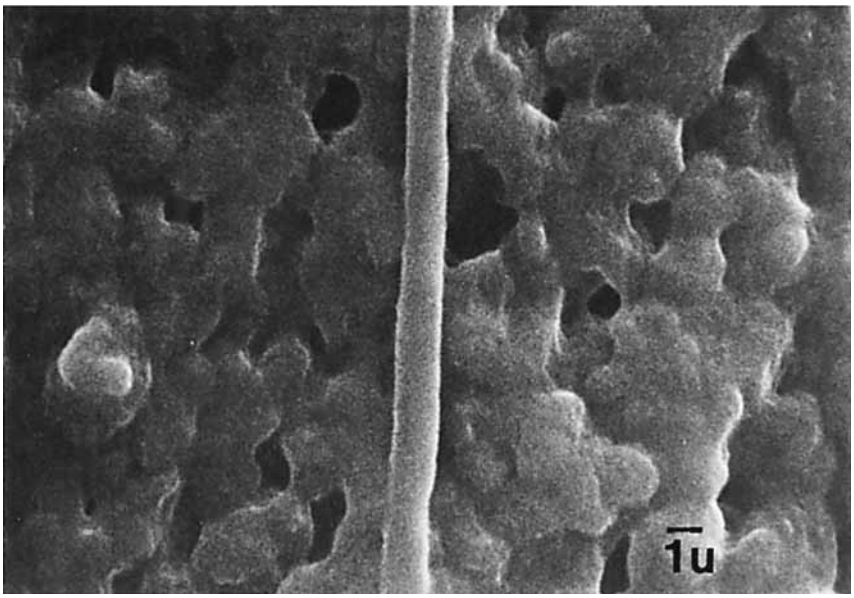

Figure 15 High magnification SEM micrograph of Triad2 (2 : 6 : 7) fibril after solvent etching the PET matrix.

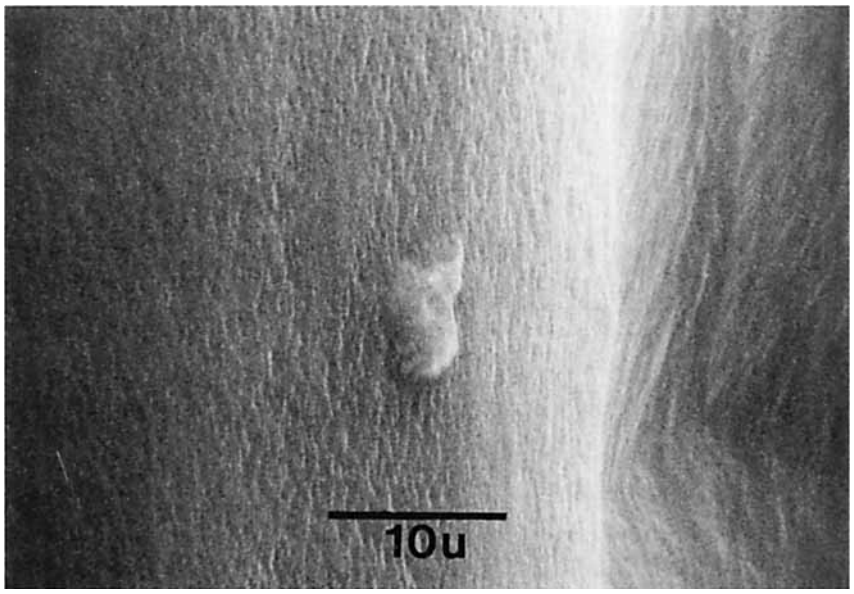

Figure 16 SEM micrograph of the solvent etched PET control fiber.

removed in an uneven fashion during the etching process. The Triad2 (2 : 6 : 7) may also be modifying the PET matrix slightly, causing a change in the fiber's solubility. The extent of interaction between blend components is not yet known but partial miscibility or compatibility is considered a significant possibility, particularly since a large portion of LCP cannot be accounted for at this point. Digital analysis of fiber cross sections indicates only 7% to 12% block copolymer phase within the fiber, neglecting the 1-μm skin region. Furthermore, examples of partial miscibility between thermotropic polyesters and PET are prevalent in the literature although the type and extent of interaction has not been adequately studied.[10,28–32]

The morphology of the as-spun fibers is further evidence that the Triad2 (2 : 6 : 7) polymer may not have remarkable properties. Although fibrillation of the Triad2 (2 : 6 : 7) phase was achieved, mechanical reinforcement of the PET was not observed. It is possible that the number of fibrils or their aspect ratios was insufficient to enhance the as-spun fibers but this is unlikely, particularly at the 20 wt % loading level. A more reasonable suggestion is that the inherent mechanical properties of the Triad2 (2 : 6 : 7) are poor. Thus the block copolymer phase cannot mechanically contribute to the improvement of the PET matrix.

The possibility that the posttreatment improves the mechanical performance of the Triad2 (2 : 6 : 7) cannot be completely discounted at this point. Drawing could affect the Triad2 (2 : 6 : 7) phase in the following ways: 1) improved orientation of the block copolymer material, i.e., a greater number of fibrils with higher aspect ratios may develop; 2) failure of the Triad2 (2 : 6 : 7) phase, i.e., breakup of the existing fibrils; and 3) the block copolymer may remain unchanged. Unfortunately, due to the high degree of crystallinity in the drawn fibers and the similarity of molecular architecture between the two blend components, attempts to distinguish between the phases by solvent etching were not successful. Thus the Triad2 (2 : 6 : 7) block copolymer phase could not be identified in the drawn fibers. Future work will focus on developing a model system to examine the drawing process in these blends and on determining the true mechanism responsible for the reinforcement of the drawn fibers.

CONCLUSIONS

Improving blend compatibility should increase the interfacial adhesion between the different components and thus the mechanical performance. This investigation has focused on using liquid crystalline block copolymers as a means of improving the compatibility between a rigid mesogen and PET. Several different block copolymers have been screened in an effort to determine the optimum molecular architecture necessary to attain good compatibility and ultimately provide reinforcement of PET fibers. Examined variables included wt % rod content, PBT block size, and rigid-rod block size.

The quantity of PBT incorporated into the polymer chain had little effect on tensile performance

but dramatically influenced the thermal stability. Decreasing the length of the PBT moieties reduced the amount of free shrinkage exhibited by the blended fibers. The length and type of mesogen incorporated influenced both the tensile and thermal behavior of the posttreated systems. The stiffer Triad2 mesogen was more effective than Triad4 at improving the mechanical performance of the fibers, particularly when longer mesogenic blocks were used. At the 20 wt % loading level, the Triad2 systems exhibited both strength and stiffness characteristics significantly greater than the PET control.

Currently the mechanism of reinforcement in the Triad2 blends is unclear. The as-spun fibers did not exhibit any property improvements, despite fibrillation of the block copolymer phase. Increases in mechanical and thermal performance were observed only after posttreatment, indicating a modification of the PET matrix rather than mechanical reinforcement. Partial miscibility or interaction between the copolymer and PET is considered a possibility, since all of the block copolymer could not be accounted for using microscopy; however, evidence of good adhesion between the two phases could not be observed.

Although the mechanism of improvement is currently unknown, it is obvious that the addition of mesogenic block copolymers can significantly enhance the performance of PET. This is an important accomplishment, since PET fibers must undergo extensive post-treatment in order to attain the necessary performance characteristics. At comparable loading levels, conventional thermotropic LCP's would embrittle the PET matrix to such an extent that post-treatment would not be possible. Another advantage of these block copolymers is the onset of liquid crystallinity at lower temperatures, permitting greater processing flexibility. Thus the potential of these materials is high, particularly since the processing conditions could not be optimized due to material constraints. By continuing to modify the molecular architecture and processing of these block copolymers, greater improvements in fiber performance are expected.

REFERENCES

1. G. Kiss, *Polym. Eng. Sci.*, **27,** 410 (1987).
2. K. G. Blizard and D. G. Baird, *Polym. Eng. Sci.*, **27,** 653 (1987).
3. P. Zhuang and T. Kyu, *Polym. Commun.*, **29,** 99 (1988).
4. B. Lee, *Polym. Eng. Sci.*, **28,** 1107 (1988).
5. M. R. Nobile, E. Amendola, L. Nicolais, D. Acierno, and C. Carfagna, *Polym. Eng. Sci.*, **29,** 244 (1989).
6. W. Brostow, *Polymer*, **31,** 979 (1990).
7. D. Dutta, H. Fruitwala, A. Kohili, and R. A. Weiss, *Polym. Eng. Sci.*, **30,** 1005 (1990).
8. V. G. Kulichikhin and N. A. Plate, *Polym. Sci. USSR*, **33,** 1 (1991).
9. S. H. Jung and S. C. Kim, *Polym. J.*, **20,** 73 (1988).
10. P. Zhuang, T. Kyu, and J. L. White, *Polym. Eng. Sci.*, **28,** 1095 (1988).
11. G. Crevecoeur and G. Groeninckx, *Polym. Eng. Sci.*, **30,** 532 (1990).
12. B. R. Bassett and A. F. Yee, *Polym. Compos.*, **11,** 10 (1990).
13. F. Ignatious, S. W. Kantor, and R. W. Lenz, *Proc. ACS Div. Polym. Chem., ACS*, **34,** 1586 (1993).
14. C. Ober, W. Lenz, G. Galli, and E. Chiellini, *Macromolecules*, **16,** 1034 (1983).
15. I. Francis, W. Lenz, and S. Kantor, private communication.
16. A. Bilibin, A. Ten'kovtsev, O. Piraner, and S. Skorokhodov, *Polym. Sci. USSR*, **26,** 2882 (1984).
17. G. Allen, J. C. Benington, and L. S. Aggarwal, ed., *Comprehensive Polymer Science*, Vol. 7, Pergamon Press, New York, 1989, p. 249.
18. S. D. Long and I. M. Ward, *J. Appl. Polym. Sci.*, **42,** 1921 (1991).
19. B. Shin and I. Chung, *Polym. Eng. Sci.*, **30,** 13 (1990).
20. B. Shin and I. Chung, *Polym. Eng. Sci.*, **30,** 22 (1990).
21. J. Li, M. Silverstein, A. Hiltner, and E. Baer, *J. Appl. Polym. Sci.*, **44,** 1531 (1992).
22. M. Heino and J. Seppala, *J. Appl. Polym. Sci.*, **44,** 2185 (1992).
23. B. Shin, S. Jang, I. Chung, and B. Kim, *Polym. Eng. Sci.*, **32,** 73 (1992).
24. M. Kyotani, A. Kaito, and K. Nakayama, *Polymer*, **33,** 4756 (1992).
25. O. Federico, *In-Situ Composites of a Thermotropic Liquid Crystalline Polymer and Polycarbonate: Processing, Morphology and Properties*, Ph.D. Thesis, University of Massachusetts, Amherst, 1989.
26. A. Mehta and A. I. Isayev, *Polym. Eng. Sci.*, **31,** 971 (1991).
27. A. M. Sukhadia, D. Done, and D. G. Baird, *Polym. Eng. Sci.*, **30,** 519 (1990).
28. M. Kimura and R. S. Porter, *J. Polym. Sci.*, Polym. Phys. Ed., **22,** 1697 (1984).
29. A. Ajji, J. Brisson, and Y. Qu, *J. Polym. Sci., Part B*, **30,** 505 (1992).
30. W. N. Kim and M. M. Denn, *J. Rheol.*, **36,** 1477 (1992).
31. W. H. Jo, H. Yim, I. H. Kwon, and T. W. Son, *Polym. J.*, **24,** 519 (1992).
32. A. Ajji and P. A. Gignac, *Polym. Eng. Sci.*, **32,** 903 (1992).

Received November 15, 1993
Accepted March 11, 1994